Automated Segmentation of SAS Images using the Mean – Standard Deviation Plane for the Detection of Underwater Mines

Frédéric Maussang[a], Jocelyn Chanussot[a] & Alain Hétet[b]
[a]Laboratoire des Images et des Signaux - CNRS
LIS / ENSIEG – Domaine Universitaire – BP 46
38402 Saint-Martin-d'Hères Cedex, France
{frederic.maussang ; jocelyn.chanussot}@lis.inpg.fr

[b]Groupe d'Etudes Sous-Marines de l'Atlantique – DGA/DCE/GESMA
BP 42
29240 Brest Naval, France
hetet@gesma.fr

***Abstract-* A segmentation method of synthetic aperture sonar (SAS) images is presented, in order to highlight some characteristics (number, position, shape, …) of underwater mines echoes. This segmentation method is based on statistical characteristics of the sonar images, highlighted by the mean – standard deviation plane. It is automated by using an entropy criterion.**

I. INTRODUCTION

The detection and classification of different types of underwater mines is a present crucial strategic task [1]. Over the past few years, synthetic aperture sonar (SAS) has been increasingly used in sea bed imagery, and the high resolution images provided can be used for this purpose. Indeed, being composed of an active sonar moving along a nominally straight rail, it permits to simulate a long antenna, which would be impossible to build because of its high cost and for technical reasons.

After a classical processing, the beam-forming, permitting to combine coherently the signals recorded at different positions, and delay compensation, a sonar image representing the sea bed is obtained. Interesting information can be extracted from this image.

The real data processed and presented in this paper have been recorded during the IFSAS'99 experiment in the context of a collaboration between the DGA (Délégation Générale pour l'Armement, France) and the DERA (Defense Evaluation and Research Agency, United Kingdom) which provided and operated the experimental equipment. An image of the sea bed is obtained representing a region of 10m x 20m with a resolution of approximately 1cm in both dimensions (Fig. 1). It contains two mines which can be seen thanks to the shadows projected on the sea bed and the echoes (specular reflections in front of the shadows). In this paper, results will be presented on the part of the image containing the "rockan" mine.

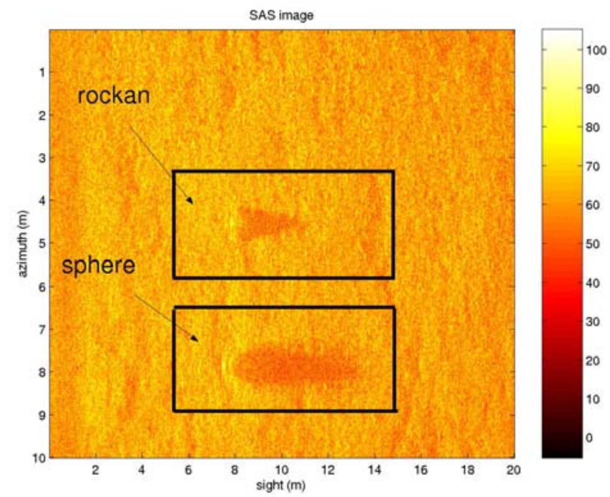

Fig. 1. Image obtained after SAS data processing (dB scale).

II. STATISTICAL PROPERTIES

A. Speckle Noise and Rayleigh Law

The sonar images provided by the SAS system are seriously corrupted by a speckle noise which gives to the image its granular aspect. This noise comes from the presence of elements (sand, rocks, …) that are smaller than the used wave length. These elements are supposed to be randomly distributed on the sea bed. Therefore, the sensor records the result of the interference of all the waves reflected by these diffusers contained in a resolution cell [2][3].

The response ρ on a resolution cell can then be described by the following equation:

$$\rho = A.\exp(j.\phi) = X + j.Y \tag{2.1}$$

with X and Y gaussian random values.

The amplitude $A=\sqrt{X^2+Y^2}$ being the interesting parameter here, its probability density function is evaluated. A Rayleigh law is obtained [4]:

$$ {}_{A}(A)=\frac{A}{\alpha^2}\exp\left(-\frac{A^2}{2\alpha^2}\right)\ ;\ A\geq 0 \tag{2.2}$$

The ν^{th} order moment of A follows the equation:

$$E(A^\nu)=(2\alpha^2)^{\nu/2}\Gamma(1+\frac{\nu}{2}) \tag{2.3}$$

This formula results in an interesting property of the Rayleigh law which is the proportionality relationship between the standard deviation σ_A and the mean μ_A of the amplitude A:

$$\mu_A=k_R.\sigma_A \quad \text{with } k_R\approx 1.91 \tag{2.4}$$

B. Weibull Law

The previous description of the speckle noise is the most usual. But it is not always satisfactory when compared with the experience, in particular when a significant decrease of the diffusers number in a resolution cell is observed. This case is frequently seen in high resolution images [3]. Then the amplitude A of the signal is described by a Weibull law:

$$ {}_{A}(A)=\frac{\delta}{\beta}\left(\frac{A}{\beta}\right)^{\delta-1}\exp\left\{-\left(\frac{A}{\beta}\right)^{\delta}\right\}\ ;\ A\geq 0 \tag{2.5}$$

The parameter δ, which is estimated on the sonar image with a maximum likelihood estimator [5], makes this law more flexible than the Rayleigh law (a special case with $\beta=\sqrt{2}\alpha$ and $\delta=2$).

The performance of this modeling can be estimated on the histogram and quantified by a χ^2 criterion or Kolmogorov distance [5]. The χ^2 criterion d_{χ^2} is estimated according to the relation:

$$d_{\chi^2}=\sum_{i=1}^{r}\frac{(k_i-nP_i)^2}{nP_i} \tag{2.6}$$

with k_i being the number of realizations and P_i the probability estimated of the value i, r the number of possible values and n the number of observations (pixels in our case). The Kolmogorov distance K is defined by:

$$K=\sum_{i=1}^{r}\left|k_i-nP_i\right| \tag{2.7}$$

the parameters having the same definition as before. Fig. 2 shows how each law can describe efficiently the distribution of values in the background noise of the image containing the "rockan" mine, the parameters of the laws being estimated with a maximum likelihood estimator. A quantified comparison is made on Tab. 1. Then we can see that a Weibull law describes more efficiently the sonar image than a Rayleigh law.

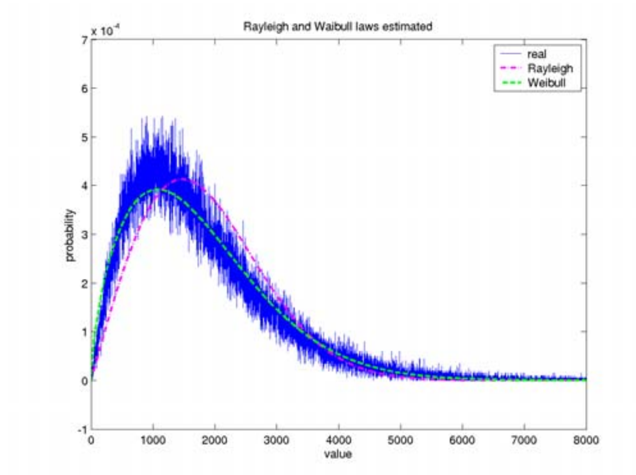

Fig. 2. Rayleigh law (plotted and dashed line) and Weibull law (dashed line) estimated on pixels values distribution (continuous line).

TABLE I
COMPARISON OF THE PERFORMANCES OF THE LAWS ON THE "ROCKAN" IMAGE

Law	Criterions	
	χ^2 criterion	Kolmogorov distance
Rayleigh	1.98	0.251
Weibull	0.0883	0.147

For a Weibull law the ν^{th} order moment of A is:

$$E(A^\nu)=\beta^\nu\Gamma\left(1+\frac{\nu}{\delta}\right) \tag{2.8}$$

Therefore, with this law, the relationship between σ_A and μ_A is preserved, but with a coefficient $k_W(\delta)$ depending of δ:

$$k_W(\delta)=\frac{\Gamma\left(1+\frac{1}{\delta}\right)}{\sqrt{\Gamma\left(1+\frac{2}{\delta}\right)-\Gamma\left(1+\frac{1}{\delta}\right)^2}} \tag{2.9}$$

This property, which leads to consider the speckle as a multiplicative noise, will be used in the continuation for the segmentation of the sonar images.

C. Speckle Processing

A plentiful literature deals with processing of images corrupted by the speckle noise. A lot of domains are concerned like sonar imagery [4][5][6], but also radar imagery [7] or medical imaging [2] too.

Among all the processes proposed by the scientists, some are based on the multiplicative property of the speckle (2.4) they try to smooth. Lee's filter is one of the most classical examples [8]. This filter is based on the local evaluation of the mean and standard deviation on the sonar image. Homomorphic filters [9] turn multiplicative noise into additional noise (with the logarithm) in order to use common filters for additive noise (mean filter, median filter, …).

In the context of mine hunting, former studies tried to segment and study the projected shadows using a markovian modeling of the sonar image [3][4][5].

In this paper, we want to carry out a segmentation of the mines echoes using local statistical characteristics of the SAS image, in order to highlight regions of interest for a detection and classification of underwater mines. In order to preserve the statistical information of the image, described in the previous section, no filtering is performed on the original image.

III. MEAN – STANDARD DEVIATION REPRESENTATION

Recent studies [10] proved the interest of the projection of a sonar image on a mean – standard deviation plane. This enables the separation of the echoes from the background noise, thanks their respective different statistical characteristics: noise and shadows are of low means and low standard deviations, whereas the echoes, deterministic elements, are of high means and low standard deviation, with a transition of high standard deviation and increasing mean.

Fig. 3 shows the mean – standard deviation representation of the image containing the "rockan" mine (Fig. 4). After local estimation of mean and standard deviation on a 5x5 neighborhood, each pixel is represented by a point on the mean – standard deviation plane. The dimensions of the square sliding filtering window must be chosen by taking into account that low dimensions leads to a high variance on the estimation, and high dimensions make the deterministic structure become bogged down in the background noise.

Then, a linear structure can be seen, corresponding to the proportionality relationship between mean and standard deviation previously mentioned. The structures looking like "horns" correspond to the echoes on the sonar image. So several "horns" can be seen at different positions and are of different dimensions, each one corresponding to one specific echo. These characteristics can then permit, relatively easily, to differentiate each echo from the other, and from the background noise, for which the corresponding points on the representation are close to the origin.

IV. SEGMENTATION

A. Description of the Segmentation Method

In order to highlight some characteristics of the echoes and to locate regions of interest for the detection and the classification of these mines, a segmentation of the sonar image is performed with a simple threshold in the mean – standard deviation plane.

The principle of the method used in this paper comes from the observation made before: it is relatively simple to locate the pixels of noise because their representation in the mean – standard deviation plane is close to the origin. Therefore the idea is to isolate these points by using thresholds both in standard deviation and in mean, and to put the corresponding pixels on the image to zero (the other are put to 1). The proportionality relationship between the mean and the standard deviation of the noise (2.4) permits to estimate the threshold in mean when a threshold in standard deviation is fixed.

To estimate the proportionality coefficient and derive the value of one threshold from the other, three solutions can be investigated :

- we choose the coefficient evaluated by the Rayleigh law (≈ 1.91, (2.4)) and the threshold in mean is estimated with this factor,
- or we choose the coefficient evaluated by the Weibull law (2.9),
- or the regression line is estimated by a mean square method and the threshold in mean is calculated as the image of the threshold in standard deviation by this line.

With a linear regression on the mean – standard deviation representation of the "rockan" image (Fig. 3), a line with a slope of approximately 1.57 is obtained. The difference between this value and the coefficient evaluated by the Rayleigh law comes from the borderlines of the statistical modeling of the noise by this law. A description with a Weibull law gives a coefficient closer from the result of the linear regression (same value with an approximation of 10^{-2}).

The last solution is chosen here for the segmentation, with a regression line represented with a dashed line and the thresholds with thick lines (Fig. 3). The result of the segmentation can be seen on Fig. 5 with the segmented echoes of the mine appearing clearly.

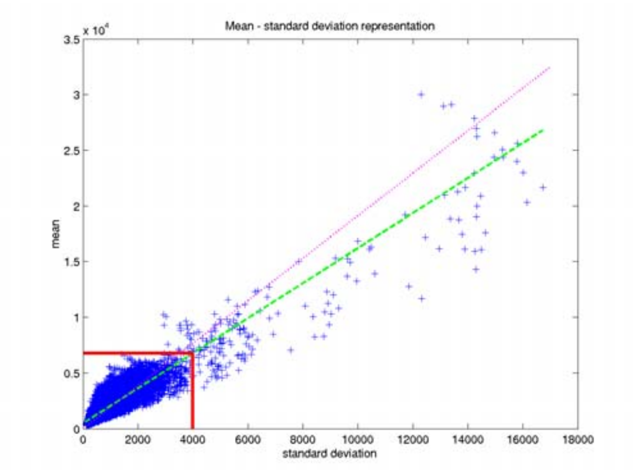

Fig. 3. Mean - standard deviation representation: comparison between the proportionality relations by Rayleigh (plotted line) and by Weibull or linear regression (dashed line) and representation of the thresholds for the segmentation (standard deviation: 4000; mean: 6751).

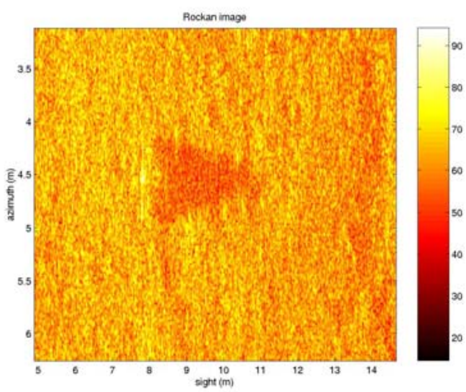

Fig. 4. "Rockan" image.

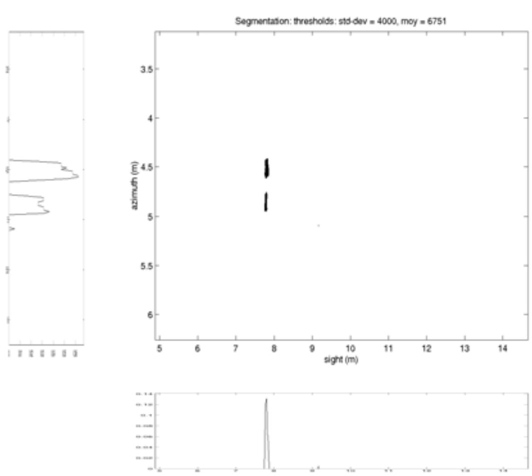

Fig. 5. Segmented "rockan" image and repartition of the segmented pixels according to both axes. Calculated entropies: X-axis: 3.46; Y-axis: 4.58.

B. *Automation of the Segmentation using an entropy criterion*

In the previous section, we have seen a segmentation method where a threshold in standard deviation is fixed by the operator, the threshold in mean being evaluated from this value. In this paper, an automation of the segmentation method is proposed in order to adjust this threshold automatically. To reach this goal, a progressive segmentation is performed by progressively increasing the threshold in standard deviation. To stop the process and determine the final threshold value, the entropy with respect to both axis of the segmented image is studied. This entropy is evaluated by counting the number of segmented pixels column by column (respectively line by line) on the X-axis (respectively Y-axis), and the results are normalized to 1 in order to consider the results as probability density functions (Fig. 5). Then the entropy H_{axis} on each axis is calculated following :

$$H_{\text{axis}} = -\sum_{p_{\text{axis}}(i)\neq 0} p_{\text{axis}}(i).\log_2 p_{\text{axis}}(i) \ ; \ i=1\ldots N_{\text{axis}} \qquad (4.1)$$

with N_{axis} the number of columns (respectively of lines) and $p_{\text{axis}}(i)$ the "number of segmented pixels" (after normalization) in the column (respectively the line) i. These criterions permit to estimate the spreading of the segmented pixels along both axis: the higher is the entropy, the more uniformly the segmented pixels are spread out on the image (the threshold then reaches the noise level).

By performing a progressive segmentation (the threshold is progressively decreased), an increase of the entropy according to both axis can be seen, but this increase is not regular (see Fig. 6). Two slope breakings, with a neat one, can be seen on the Y-axis (azimuth), and a neat slope breaking on the X-axis (sight). The slope breaking are pointed out by arrows on Fig. 6: the slope breaking 1, only observed on the azimuth, is at a standard deviation of about 6250 and the breaking 2 at about 4000.

To understand the cause of these irregularities, different segmentations corresponding at different threshold values between the breakings are presented (Fig. 7). We can see that, when the threshold is decreasing progressively, the first echo begins to be segmented. Then the second echo begins to be segmented which explains the rapid increase of the entropy (breaking 1), the segmented pixels being assembled into two regions instead of one. Finally, the background noise is segmented, which explain the neat increase of the entropy (breaking 2). The two segmented echoes being parallel to the azimuth axis, the first slope breaking is only seen on the azimuth axis: indeed, all along the segmentation, before the background noise begins to be segmented, the sight axis only "sees" one segmented object.

Therefore the optimized segmentation, permitting to see both echoes with a maximal size, is with a threshold corresponding to the highest slope breaking. Indeed a segmentation with a lower threshold segments noise elements. The result is presented on Fig. 5 where we can see two distinct echoes, which then enables then description of the mine.

V. CONCLUSION AND PERSPECTIVES

This paper presented an automated segmentation of the SAS images using their statistical characteristics (representation in the mean- standard deviation plane). The automation of the method has been here achieved by using a criterion (the entropy) estimating the spreading of the segmented pixels over the image. This criterion permits to differentiate a segmentation of the echoes from a segmentation of the background noise.

The proposed segmentation method uses almost no prior knowledge and is fully automatic. It enables the detection of mines echoes and therefore the selection of regions of interest in the image. This result could be used in a next step aiming at classifying the detected object.

This segmentation method is relatively robust, a significant increase of the threshold does not modify significantly the result: for example, in our case, an increase of about 50% of the threshold in standard deviation preserve the number and location of the segmented objects (2 echoes). Moreover, with this method, a gain correction between the beginning and the end of the scene on the SAS image is not necessary, the variations being of sufficiently low frequency not to change the local standard deviation, which is here the main criterion. A possible improvement of the method would consist in using an anisotropic filtering window to build the mean – standard deviation representation. Indeed such a window would decrease the variance of the estimator.

Acknowledgments

This work was supported by the French National Defense Department and the French Navy (DGA/DCE/GESMA) under Grant 01-59-918.

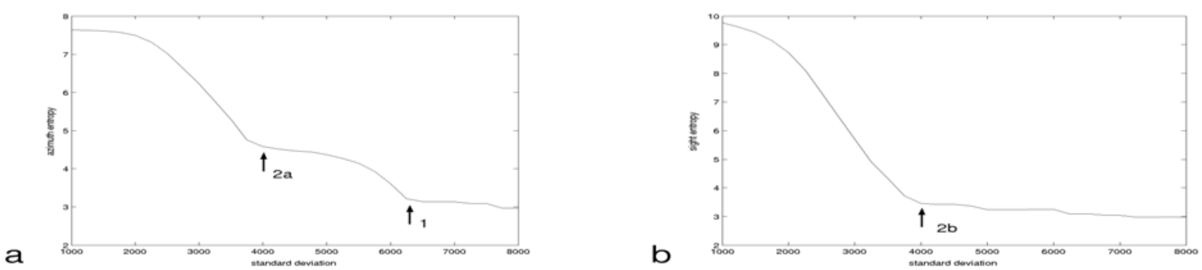

Fig. 6. Entropy variation in function of the threshold in standard deviation on the azimuth axis (a) and on sight axis (b).

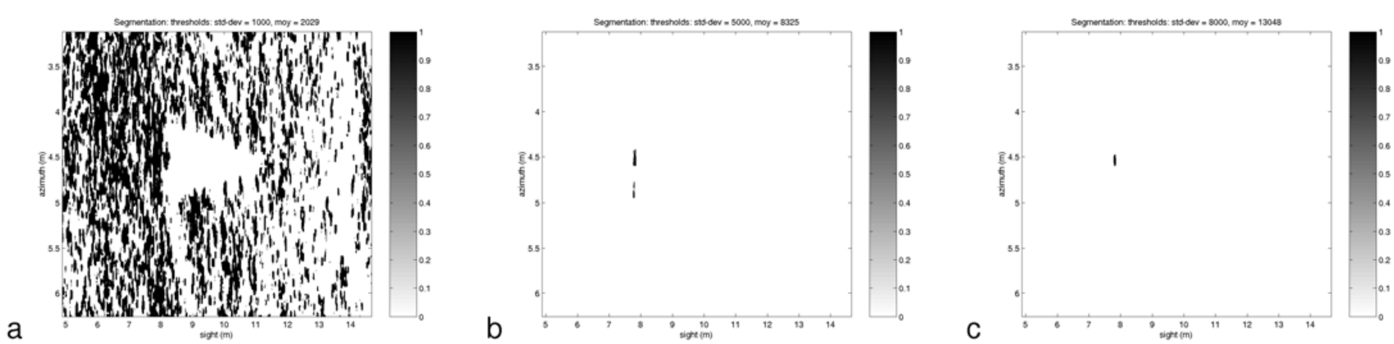

Fig. 7. Segmentation results for different thresholds in standard-deviation: 1000 (a), 5000 (b) and 8000 (c).

References

[1] J.T. Broach, R.S. Harmon, and G.J. Dobeck, conference chair of: "Detection and remediation technologies for mines and minelike targets VII", *Proc. of SPIE*, vol. 4742, sessions 9 & 10 on underwater detection, Orlando, Florida, USA, April 2002.

[2] O. Basset, "L'apport de données multimodalité et/ou multiparamétriques pour la segmentation d'images ultrasonores. Caractérisation par analyse de texture.", *HDR Université Claude Bernard – Lyon 1*, Lyon, France, July 2001.

[3] C. Collet, P. Thourel, M. Mignotte, P. Pérez, and P. Bouthemy, "Segmentation markovienne hiérarchique multimodèle d'images sonar haute résolution.", Traitement du Signal, vol. 15, n°3, pp. 231 – 250, 1998.

[4] F. Schmitt, M. Mignotte, C. Collet, and P. Thourel, "Estimation of Noise Parameters on Sonar Images", *Proc. of SPIE conference on Signal and Image Processing,* vol. 2823, pp. 1 – 12, Denver, Colorado, USA, August 1996.

[5] M. Mignotte, C. Collet, P. Pérez, and P. Bouthemy, "Three-Class Markovian Segmentation of High-Resolution Sonar Images", *Computer Vision and Image Undersatnding*, vol. 76, n° 3, pp. 191 – 204, December 1999.

[6] J. Chanussot, F. Maussang, and A. Hétet, "Scalar Image Processing Filters for Speckle Reduction on Synthetic Aperture Sonar Images", *Proc. of MTS/IEEE Oceans'02*, Biloxi, Mississippi, USA, October 2002.

[7] B. Ogor, "Etude comparative de methodes de filtrage de speckle et de segmentation en imagerie radar à synthèse d'ouverture", *Ph. D. Thesis, INSA Rennes*, Rennes, France, 1997.

[8] J.S. Lee, "Speckle analysis and smoothing of synthetic aperture radar images", *Computer graphics and image processing*, n°17, pp. 24 – 31, 1981.

[9] D. Coltuc and R. Radescu, "On the homomorphic filtering by channel's summation", *Proc. of IEEE International Geoscience and Remote Sensing Symposium (IGARSS'02)*, Toronto, Canada, June 2002.

[10] F. Maussang, J. Chanussot, C. Hory, and A. Hétet, "Synthetic Aperture Sonar Imagery: Towards a Classification of Under Water Mines in the Mean – Standard Deviation Plane", *Proc. of Physics in Signal and Image Processing (PSIP'03)*, pp. 137 – 140, Grenoble, France, January 2003.